International Journal of Precision Engineering and Manufacturing
https://doi.org/10.1007/s12541-022-00629-y

Online ISSN 2005-4602
Print ISSN 2234-7593

REGULAR PAPER

Response of Resin Coating Films Containing Fine Metal Particles to Ultrashort Laser Pulses

Ayumi Nakajima[1] · **Jiwang Yan**[1]

Received: 30 December 2020 / Revised: 14 August 2021 / Accepted: 3 February 2022

Abstract
Resin coating films are extensively used for aesthetic improvement and preventing deterioration of metal surfaces. Some of the films contain fine metal particles for the purpose of coloring. For such films, surface waviness with millimeter-scale wavelength is a significant problem because it induces visible irregularities on the surface. Conventionally, man-powered polishing has been used to planarize the waviness. However, it is labor-intensive and leads to other problems such as waste slurry disposal and embedment of abrasive grains in the film. Hence, a new method is required to eliminate the surface waviness. In this study, ultrashort pulsed laser irradiation on resin coating films is proposed. By controlling the focal position and/or scanning speed of the laser beam along the surface, protrusions are preferentially removed. Firstly, the effects of pulse width, laser fluence, and scanning speed on surface morphology were clarified. Next, the material removal mechanism was examined by elemental analysis of the surface and its cross section after irradiation. Finally, as a preliminary result of surface flattening, the arithmetic mean waviness in the wavelength range of 2.4–5.0 mm was reduced by 45.3%. This study demonstrated the feasibility of selectively removing and flattening of resin coating films by substituting laser processing for man-powered polishing.

Keywords Ultrashort pulsed laser · Resin coating film · Fine metal particle · Surface flattening · Composite material

1 Introduction

Resin coating films containing fine metal particles are extensively used for aesthetic improvement and preventing deterioration of metal surfaces [1–3]. The coating films are mainly composed of a resin component and a pigment component. The resin component provides uniform properties such as protection and adherence to the substrate. It also works as a carrier and suspending agent for the pigment component [4]. The pigment component includes fine metal or metal oxide particles with sizes of tens to hundreds of nanometers for the purpose of coloring [5].

One of the quantitative evaluation methods for aesthetics of a surface is waviness measurement [6, 7]. For resin coating films, surface waviness with a millimeter-scale wavelength is a significant problem because it induces visible irregularities on the surface [8]. This kind of surface with visible irregularities is called orange peel because of its visual similarity to the skin of an orange [9–12]. Orange peel makes the reflection from the surface blurrier and reduces its aesthetic appeal. Orange peel appears when resin coating films are applied to the surface with a spray gun [13]. The irregularities depend mainly on the viscosity, paint flow, and droplet size of the paint when it is sprayed [8, 14].

Conventionally, polishing has been performed by man power to reduce the waviness on curved surfaces, but this polishing method is a labor-intensive and skill-based process because operators adjust the polishing motion and force according to the surface condition [15]. Although research has been performed on automatic polishing technology, it requires complex control of tool trajectory, tool posture and polishing force, etc. to realize the polishing motion of skilled people [15, 16]. Moreover, it induces other problems such as waste slurry disposal and adhesion/embedment of abrasive grains to the surface. Hence, an alternative method that

This paper was presented at PRESM2020.

✉ Jiwang Yan
yan@mech.keio.ac.jp

[1] School of Integrated Design Engineering, Graduate School of Science and Technology, Keio University, Hiyoshi 3-14-1, Kohoku-ku, Yokohama 223-8522, Japan

Published online: 24 February 2022

does not require disposal of liquid waste and skilled labors is needed.

In this study, ultrashort pulsed laser irradiation is proposed to reduce the surface waviness on resin coating films. Laser processing is a non-contact method, and it is possible to remove materials locally and selectively by simple automatic operation. Besides, it has advantages of low environmental pollution, thus contributes to the realization of green manufacturing. Various pulsed laser processing methods of polymers have been investigated [17–20], for example, removal of coatings [21–24] and surface modification [25]. However, surface flattening of resin coatings containing fine metal particles has hardly been reported before, and the ultrashort pulsed laser processing characteristics and mechanisms of resin coating films containing fine metal particles have not been clarified [18].

It has been reported that for metallic materials [26] and semiconductors [27], nanosecond pulsed laser irradiation causes melting and surface tension leads to flattening. On the other hand, a recent study showed that selective and localized removal of surface protrusions by using picosecond pulsed laser irradiation also enabled metal surface flattening [28]. For this reason, it is essential to identify a suitable laser pulse width for surface flattening of a new material. In this work, firstly, basic laser processing characteristics of resin coating films containing fine metal particles were investigated by using nanosecond and femtosecond pulsed lasers to determine whether melting or preferential removal of surface protrusions was more appropriate for surface flattening by comparing the material's responses to different pulse widths. Secondly, the effects of laser fluence and scanning speed on processing depth and surface morphology were clarified. Thirdly, the material removal mechanism was examined by elemental analysis of the surface and its cross section after irradiation. Finally, surface flattening tests using the femtosecond pulsed laser were performed to examine the feasibility of the proposed method.

2 Surface Flattening Mechanism

A schematic diagram of the expected surface flattening mechanism using a femtosecond pulsed laser is shown in Fig. 1. In ultrashort pulsed laser processing, as the laser fluence gradually concentrates toward the focal point, as shown in Fig. 1a, the amount of material removal increases as the distance of the surface from the focal point decreases. Only the region where the laser fluence exceeds the ablation threshold is selectively removed. Therefore, as shown in Fig. 1b, by controlling the focal point and scanning the laser beam along the surface, surface protrusions near the focal point will be preferentially removed. This mechanism has made it possible to obtain a flat surface on metals [28],

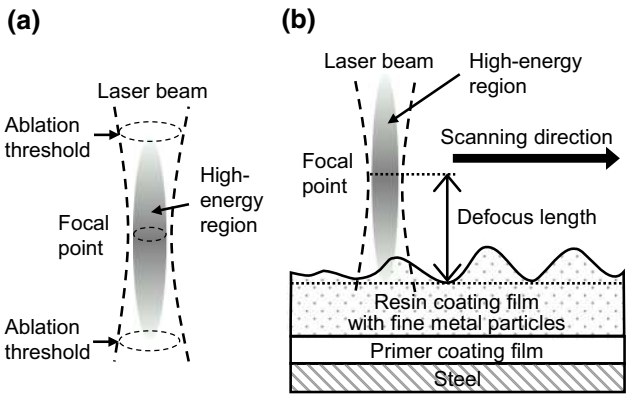

Fig. 1 Schematic diagrams of surface flattening mechanism of resin coating films containing fine metal particles by ultrashort pulsed laser irradiation: **a** laser fluence distribution within a laser beam, **b** selective removing surface protrusions by beam scanning

but it has not been applied to resin materials. In this study, the fundamental laser processing and flattening characteristics of resin coatings with metal particles were investigated.

3 Experiments

In this study, two types of lasers were used. The first one was Super Pulse 532-30, a nanosecond pulsed laser manufactured by Inngu Laser Co., Ltd., China. The laser wavelength was 532 nm and the repetition frequency was 100 kHz. The laser spot size (D) was 85 μm. The second one was PHAROS-08-600-PP, a femtosecond pulsed laser manufactured by Light Conversion, Lithuania. The laser wavelength was switchable between 514 and 1030 nm, and the repetition frequency was 100 kHz. The laser spot size was 15 μm. The laser fluence for both laser beams had a Gaussian distribution.

Resin coating films composed of polyester resin and melamine resin, and Ba- and Ti-based fine metal particles with sizes of tens to hundreds of nanometers were used as workpieces. Figure 2 shows an optical image, a scanning electron microscope (SEM) image, and a cross-sectional profile of a workpiece surface. To prepare the samples, a primer coating film was electrodeposited on a steel plate with a thickness of about 20 μm. Then, a resin coating film containing fine metal particles was electrostatically coated on the primer coating film with a thickness of about 40 μm, as schematically shown in Fig. 1b. Table 1 shows the experimental conditions. The distance between the lowest position of the resin coating film and the focal point was defined as the defocus length. The experimental setup and irradiation schemes are shown in Fig. 3. The size of area of irradiation was 5 mm × 20 mm. The laser beams were scanned by a Galvanometer scanner

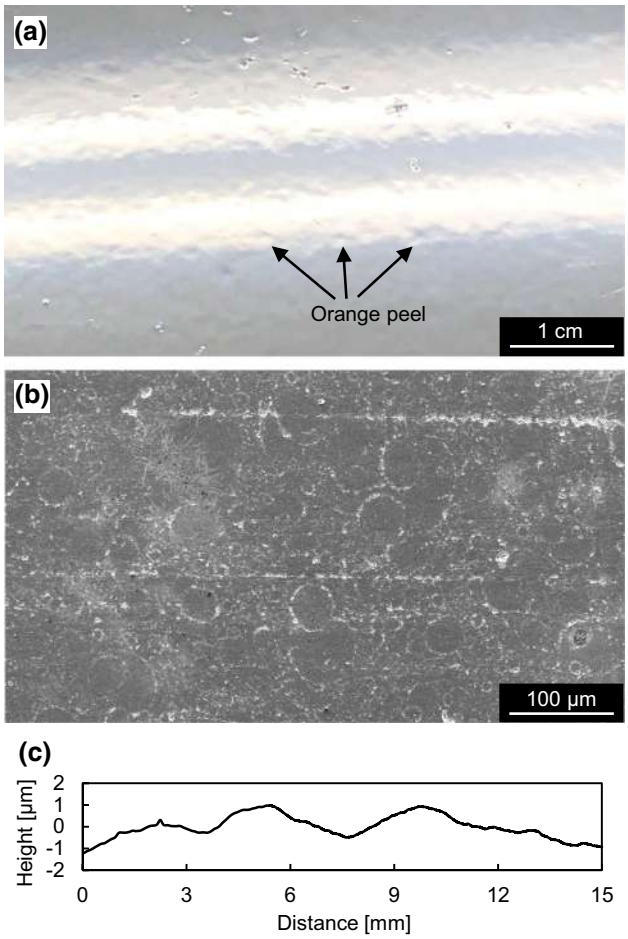

Fig. 2 Image of workpiece surface with orange peel: **a** optical image with the reflection of a light source, **b** SEM image, **c** cross-sectional profile

in X, Y directions. The workpiece height in Z direction was adjusted using a height-adjustable stage.

After the laser irradiation, the cross-sectional profile for evaluation of groove structures was measured by a laser microscope, OLS4100, made by Olympus Corporation, Japan. The 15 mm long cross-sectional profile for the waviness evaluation was measured by a two-dimensional laser probe surface profilometer, MP-3, made by Mitaka Kohki Co., Ltd., Japan. From the profile, only the waviness at the wavelength of 2.4 to 5.0 mm was extracted using the three-dimensional area measurement and analysis software Talymap Platinum 7.3, and the arithmetic mean waviness was calculated. The surface morphologies of the workpieces were observed by a SEM, Inspect F50, made by FEI Company, U.S. The cross-sectional morphologies of the workpieces were observed by another SEM, MERLIN Compact, made by Carl Zeiss, Germany. For cross-sectional SEM sample preparation, the irradiated surface was protected by another layer of resin containing Cl, and mechanical polishing was performed in a direction perpendicular to the surface. The elemental ratio was analyzed by an energy dispersive X-ray, EDAX, made by EDAX Inc., U.S.

4 Results and Discussion

4.1 Change of Surface Morphology with Pulse Width

Line irradiation was performed at a pulse width of 26 ns (laser wavelength: 532 nm) and 256 fs (laser wavelength: 514 nm), and a laser fluence of 0.5 J/cm^2. The SEM images of groove bottom surfaces irradiated with different pulse widths are shown in Fig. 4. Several holes with a diameter of about 1 μm were distributed on the surfaces for both pulse widths. When the pulse width was 26 ns, the molten resin adhered to the surface and formed irregularities. On the other hand, when the pulse width was 256 fs, particles with a diameter of approximately 1 μm were observed without adhesion of molten resin.

The change in the surface morphology with different pulse widths might be due to the difference in thermal effects [29]. When the pulse width is 26 ns, melting occurs inside the resin coating films. Heat is conducted from the laser

Table 1 Laser irradiation conditions

Laser medium	Line irradiation		Area irradiation
	Nd: YVO_4	Yb: KGW	Yb: KGW
Wavelength (nm)	532	514	514, 1030
Spot size D (μm)	85	15	15
Pulse width	26 ns	256 fs	256 fs
Repetition frequency (kHz)	100	100	100
Scanning speed V (mm/s)	200	10, 15, 30, 50, 75, 150, 300	50
Laser fluence (J/cm^2)	0.5	0.1, 0.3, 0.5, 1.0, 1.5	0.5
Number of scans	1	1	1
Defocus length (μm)	0	0	0–700
Area irradiation pitch P (μm)	–	–	10

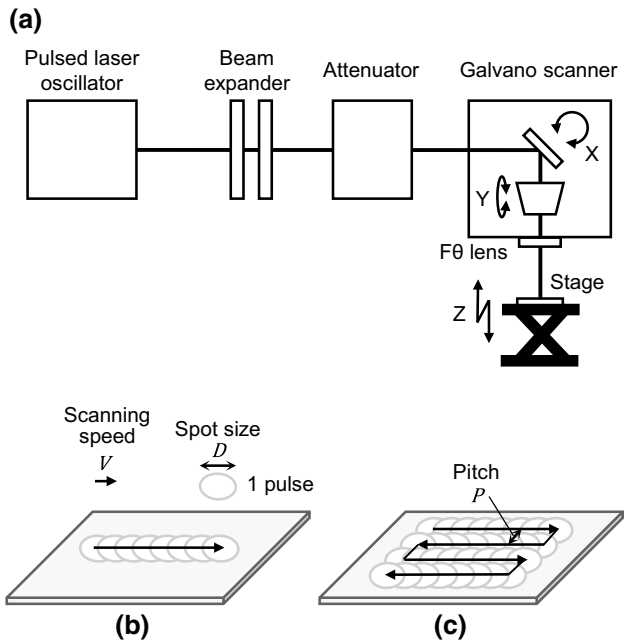

Fig. 3 Schematic diagram of experimental setup and irradiation schemes: **a** experimental setup, **b** line irradiation, **c** area irradiation

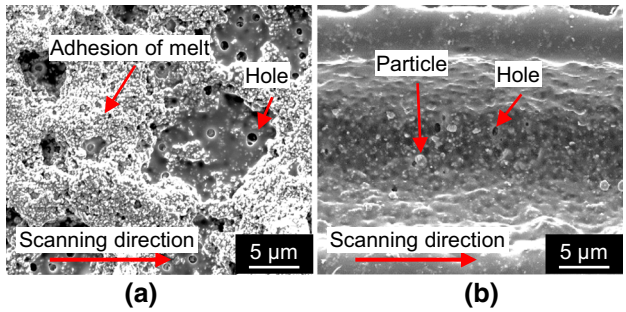

Fig. 4 SEM images of groove bottom surfaces irradiated at different pulse widths: **a** 26 ns (Scanning speed: 200 mm/s), **b** 256 fs (Scanning speed: 50 mm/s)

irradiation part to the surroundings. The heat causes partial evaporation of the pigment component including fine metal particles and thermal decomposition of the resin component. As a result, irregularities form due to adhesion of remaining molten resin. On the other hand, when the pulse width is 256 fs, the pulse duration is so short that it does not interact much with the bulk material but just with the outmost surface layer [30]. Thus, heat conduction is limited within a small area. The pigment component and the resin component are momentarily scattered and decomposed before the heat conduction spreads from the laser irradiation part to the surroundings. As a result, the molten resin does not stick to the surface because the material melting occurs only within the removed surface layer.

Compared to the nanosecond pulsed laser (26 ns), the femtosecond pulsed laser (256 fs) was found to be suitable for removing surface waviness with smaller thermal effects. Therefore, the femtosecond pulsed laser was selected in the subsequent experiments.

4.2 Change of Surface Morphology with Laser Fluence and Scanning Speed

Line irradiation was performed at a pulse width of 256 fs, and a laser wavelength of 514 nm. The SEM images of groove bottom surfaces irradiated at different laser fluence are shown in Fig. 5 (scanning speed: 50 mm/s). As the laser fluence increased, the groove width increased and the number of small holes on the groove bottoms decreased. The reason for this is that the processable area where the laser fluence exceeds the ablation threshold expands in the horizontal direction and the amount of material melting increases due to the increase in laser fluence.

The cross-sectional profiles of groove bottom surfaces irradiated at different laser fluence are shown in Fig. 6. The edge of the groove was raised higher as the laser fluence increased. This is because the molten material was swept

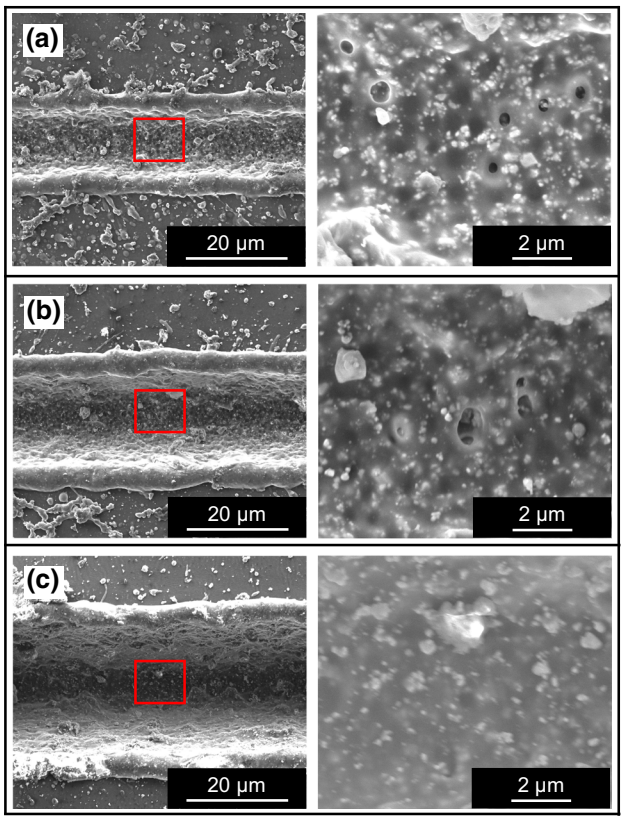

Fig. 5 SEM images of groove bottom surfaces irradiated at different laser fluence (Pulse width: 256 fs, scanning speed: 50 mm/s): **a** 0.3 J/cm^2, **b** 0.5 J/cm^2, **c** 1.0 J/cm^2

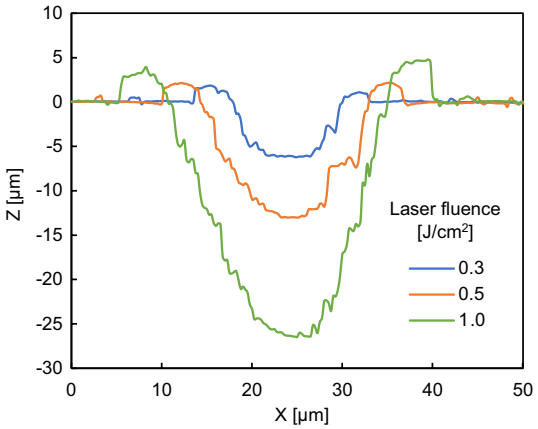

Fig. 6 The cross-sectional profiles of groove bottom surfaces irradiated at different laser fluence

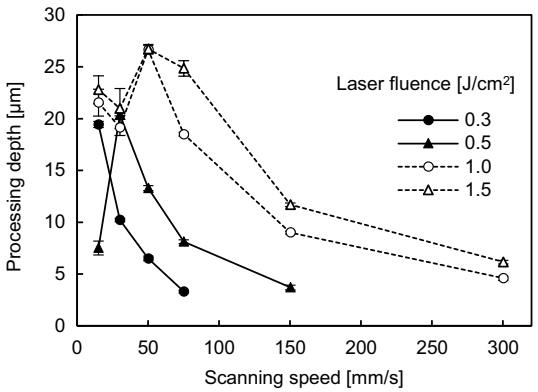

Fig. 7 The processing depth of grooves at different laser fluence and scanning speeds

outward by the recoil pressure of the material scattering near the center of the groove and then resolidified.

The processing depth of grooves irradiated at different laser fluence and scanning speeds is shown in Fig. 7. When the scanning speed was less than 50 mm/s, the depth could not be measured accurately because a large amount of debris was accumulated in the groove. As the laser fluence increased, the processing depth increased. This is because the laser beam penetrated deeper into the material as the laser fluence increased, and the ablation range became wider and the processing depth increased. In addition, the processing depth increased as the scanning speed decreased since the number of pulses per unit area increases as the scanning speed decreases.

4.3 Material Removal Mechanism

The material removal mechanism was proposed based on the observation from line irradiation results conducted at

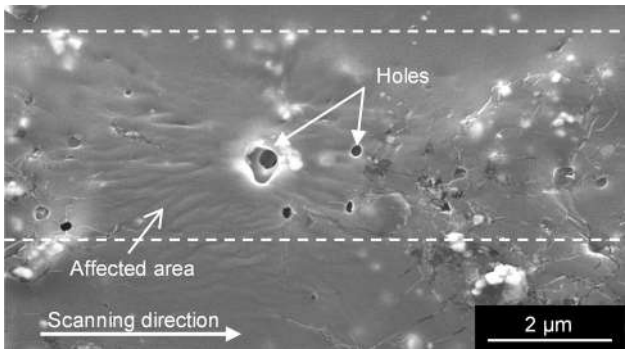

Fig. 8 SEM image of a surface irradiated at low laser fluence (0.1 J/cm^2)

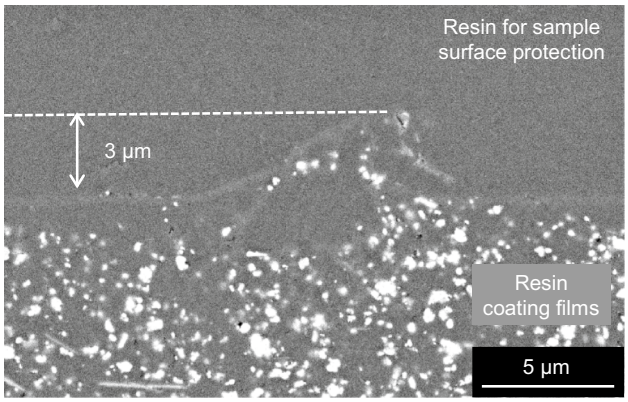

Fig. 9 Cross-sectional SEM image of a surface irradiated at low laser fluence (0.1 J/cm^2)

extremely low fluence. The irradiation was performed at a pulse width of 256 fs, a laser wavelength of 514 nm, a scanning speed of 10 mm/s, and a laser fluence of 0.1 J/cm^2. The SEM images of the irradiated surface and its cross section are shown in Figs. 8 and 9, respectively. Multiple holes were found on the irradiated surface (Fig. 8). At low laser fluence, a groove like that in Fig. 4b was not formed, but an expanded area with a height of about 3 μm was formed on the surface (Fig. 9). It was found that the fine particles that were contained in the resin coating films were not seen in the expanded area. The EDX analysis of the cross section for elements Ba and Cl is shown in Fig. 10. Inside the expanded area, there was almost no Ba that was contained in the resin coating films. Instead, a large amount of Cl was observed in the expanded area. From this result, it is presumable that the resin for the sample surface protection entered inside the expanded area through the surface holes formed by laser irradiation. In other words, a cavity was formed by laser irradiation at low laser fluence.

Next, area irradiation was performed to see the change in surface elemental ratio due to irradiation at a laser

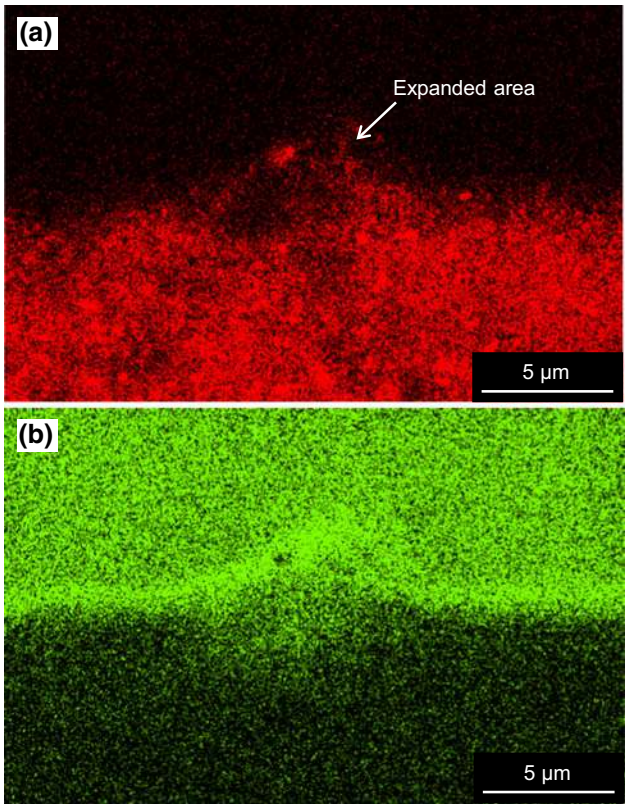

Fig. 10 EDX analysis of a cross-sectional sample of a surface irradiated at low laser fluence (0.1 J/cm^2): **a** Ba, **b** Cl

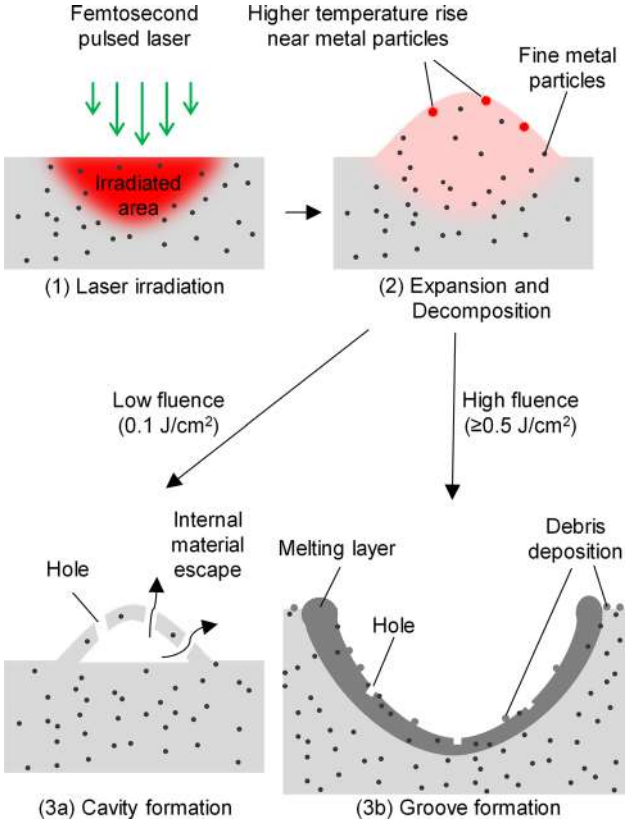

Fig. 12 Schematic of material removal mechanism for resin coating film containing fine metal particles by femtosecond pulsed laser irradiation: (*3a*) low fluence (0.1 J/cm^2), (*3b*) high fluence (≥ 0.5 J/cm^2)

wavelength of 514 nm, a pulse width of 256 fs, a scanning speed of 50 mm/s, a laser fluence of 0.5 J/cm^2, and a defocus length of 500 μm. The EDX analysis result of the surface before and after irradiation is shown in Fig. 11. After irradiation, the proportion of C decreased, and the proportion of other elements increased. In particular, the proportion of metallic elements included in the pigment component such as Ba and Ti increased significantly. This might be because the thermal decomposition temperature of the resin component is much lower than the melting point of the pigment component, so that the resin component is preferentially removed, resulting in an increase in the proportion of metallic elements.

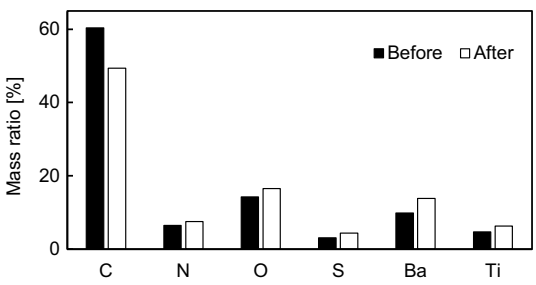

Fig. 11 EDX analysis of the surface before and after irradiation

Based on these results, the material removal mechanism of the resin coating film containing fine metal particles by femtosecond pulsed laser irradiation was discussed as shown in Fig. 12. The response of the coating film to laser irradiation is dependent on the difference in thermal conductivity and specific heat capacity between the resin coating film and the fine metal particles. The thermal conductivity of the resin is lower than that of the metal, and the specific heat capacity of the metal is smaller than that of the resin. Consequently, the surface temperature of fine metal particles will rise higher than that of the resin during laser irradiation. The temperature of the resin near the metal particles rises rapidly and the resin near the particles expands and decomposes into polymer fragments easier than other parts of resin. Hence, holes are formed near the metal particles. At low laser fluence (0.1 J/cm^2), the internal material escapes as polymer fragments from the holes on the surface, and a cavity is formed by cooling without removing the surface layer [Fig. 12(3a)]. There is insufficient internal pressure to remove the surface layer since the laser fluence is low. On the other hand, at a high laser fluence (≥ 0.5 J/cm^2), the

irradiated part expands more rapidly to a larger size, the entire expanded part including the surface layer is removed since there is enough internal pressure. Then a groove like that in Fig. 4b is formed and particles with a diameter of approximately 1 μm are deposited as debris on the surface [Fig. 12(3b)]. It is thought that this debris is composed mainly of fine metal particles.

4.4 Reduction of Waviness by Defocusing

Based on the investigation of the laser processing characteristics of resin coating films, surface flattening was performed. As the Rayleigh length is shorter, the gradient of the laser fluence is larger in the beam and more effective reduction of waviness might be performed due to the mechanism mentioned in Sect. 2. Therefore, a laser wavelength of 1030 nm was used in the surface flattening tests because the Rayleigh length halves when the laser wavelength doubles. In order to find the effect of defocusing on surface flattening, the defocus length was changed from 0 to 700 μm, and laser fluence was set to 0.5 J/cm^2. Area irradiation was performed at a pulse width of 256 fs, a scanning speed of 50 mm/s to remove surface protrusions. The processing depths of the surfaces irradiated at different defocus lengths are shown in Fig. 13. In the figure, the processing depths for defocus lengths 0-500 μm were the averages of six cross-sectional profiles, while those for defocus lengths 600 and 700 μm were the averages of three cross-sectional profiles, respectively. The processing depth decreased as the defocus length increased due to the energy distribution in the laser beam. In the laser beam, the laser fluence is highest at the focal point where the beam diameter is smallest. As the defocus length increases, the beam diameter increases and the laser fluence at the processing point decreases, so that the amount of removed material decreases.

Next, the arithmetic mean waviness of the surface was measured at the wavelength of 2.4 to 5.0 mm which is related to orange peel. The arithmetic mean waviness at different defocus lengths is shown in Fig. 14. At a defocus length of

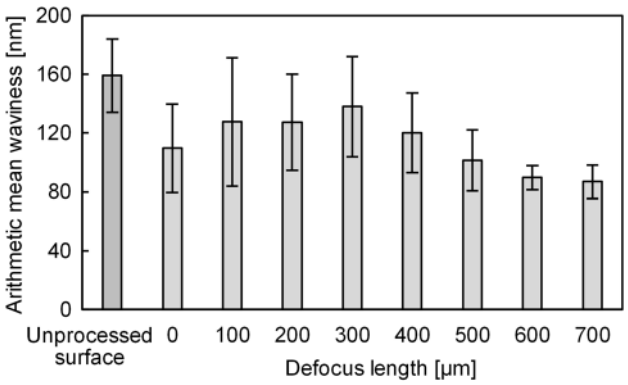

Fig. 14 Arithmetic mean waviness at different defocus lengths

500–700 μm, the reduction of waviness was confirmed as compared to the unprocessed surface (159.1 nm). In particular, the waviness was minimum (87.0 nm) and 45.3% lower than that of the unprocessed surface when the defocus length was 700 μm. This result demonstrates that by controlling the focal position, the surface protrusions were preferentially removed, as schematically shown in Fig. 1b.

The SEM images of a laser-irradiated surface with waviness removed at a defocus length of 600 μm are shown in Fig. 15 at different magnifications. On the irradiated surface, there were no marks of sprayed paint droplets that were observed on the original surface (Fig. 2b). Although small holes with a size of ~ 1 μm were seen on the surface, and the surface roughness in microscale wavelength still exists, they will not affect the aesthetic property of the surface.

5 Conclusions

Pulsed laser irradiation was performed on resin coating films containing fine metal particles to investigate the fundamental processing characteristics, mechanisms, and optimal conditions to reduce the surface waviness with a millimeter-scale wavelength.

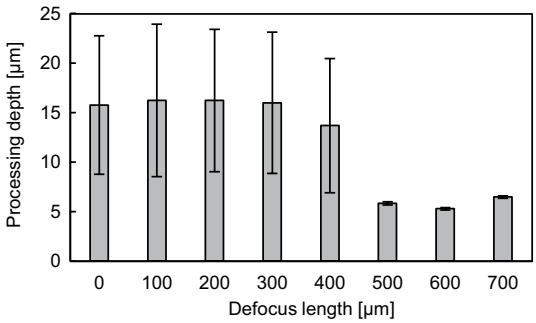

Fig. 13 Processing depth at different defocus lengths

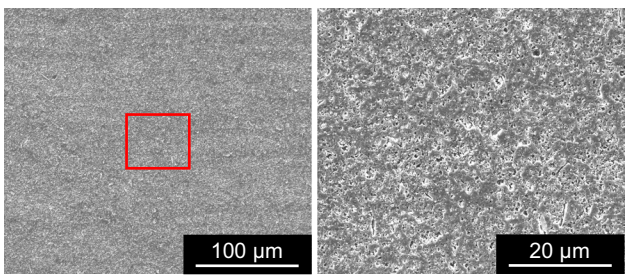

Fig. 15 SEM image of the surface after surface flattening

(1) Compared to nanosecond (26 ns) pulsed laser, femtosecond (256 fs) pulsed laser was found to be more suitable for removing the surface waviness with smaller thermal effects. At a pulse width of 256 fs, the molten material adhesion phenomenon that was observed at a pulse width of 26 ns did not occur.
(2) The effects of laser fluence and scanning speed on the processing depth, width, and surface morphology were clarified by line irradiation experiments.
(3) The elemental analysis of the sample surface and cross section after laser irradiation confirmed the expansion of the resin coating film and preferential removal of the resin component while the metal particles were deposited on the surface.
(4) The effect of defocusing on reducing the waviness was confirmed at a defocus length of 500–700 µm. The arithmetic mean waviness was reduced by 45.3% when irradiation was performed at a laser wavelength of 1030 nm, a pulse width of 256 fs, a scanning speed of 50 mm/s, laser fluence of 0.5 J/cm^2, and a defocus length of 700 µm.

Resin coating films containing fine metal particles are composite materials composed of resin and pigment, the laser processing mechanism of which is very complicated. However, the results from this study demonstrated the possibility of surface flattening by optimizing the irradiation conditions of a femtosecond pulsed laser. In this study, the Rayleigh length of the laser beam used was quite long and the waviness reduction effect was not fully exerted. Future work requires the optimization of laser beam profile and Rayleigh length as well as precise control of local dwelling time of the laser spot over the surface.

References

1. Dumont-Bècle, P., Ferley, E., Kemeny, A., Michelin, S., & Arquès, D. (2001). Multi-texturing approach for paint appearance simulation on virtual vehicles. *Sophia Antipolis*.
2. Lawman, S., Zhang, J., Williams, B. M., Zheng, Y., & Shen, Y.-C. (2017). Applications of optical coherence tomography in the non-contact assessment of automotive paints. *Optical Measurement Systems for Industrial Inspection X*. https://doi.org/10.1117/12.2270020
3. Demirci, M., & Bağcl, M. (2018). Investigation of automotive primer and basecoat paint surface's adhesion by solid particle erosion. *AIP Conference Proceedings*. https://doi.org/10.1063/1.5034542
4. Deyab, M. A., Mele, G., Al-Sabagh, A. M., Bloise, E., Lomonaco, D., Mazzetto, S. E., & Clemente, C. D. S. (2017). Synthesis and characteristics of alkyd resin/M-Porphyrins nanocomposite for corrosion protection application. *Progress in Organic Coatings, 105*, 286–290. https://doi.org/10.1016/j.porgcoat.2017.01.008
5. Lambourne, R., & Strivens, T. A. (1999). *Paint and surface coatings theory and practice*. Woodhead Publishing.
6. Sugiura, K. (2007). Study on quantitative evaluation of surface micro-smoothness in coating films. *Study of Paint, 148*, 2–9.
7. Mirjalili, F., Moradian, S., & Ameri, F. (2014). A new approach to investigate relationships between certain instrumentally measured appearance parameters and their visually perceived equivalents in the automotive industry. *Journal of Coatings Technology and Research, 11*(3), 341–350. https://doi.org/10.1007/s11998-013-9544-9
8. Kang, H., Butler, C., & Yang, Q. (1999). Evaluation of metal texture effect on paint appearance. *Three-Dimensional Imaging, Optical Metrology, and Inspection V, 3835*, 202–209. https://doi.org/10.1117/12.370262
9. Yimit, A., Itou, A., Matsui, Y., & Akashi, T. (2019). Automatic visual inspection method for a coated surface having an orange peel effect. *IEEJ Transactions on Electrical and Electronic Engineering, 14*(3), 433–440. https://doi.org/10.1002/tee.22824
10. Fernholz, K. D. (2013). Quantifying the visibility of surface distortions in class "A" automotive exterior body panels. *Journal of Manufacturing Science and Engineering*. https://doi.org/10.1115/1.4007984
11. Jafari, R., & Ameri, F. (1998). Effect of orange peel attribute of automotive finishes on their blackness perception. *Journal of Coatings Technology and Research, 15*(5), 1003–1011. https://doi.org/10.1007/s11998-018-0046-7
12. Mirjalili, F., Moradian, S., & Ameri, F. (2014). Derivation of an instrumentally based geometric appearance index for the automotive industry. *Journal of Coatings Technology and Research, 11*(6), 853–864. https://doi.org/10.1007/s11998-014-9608-5
13. Konieczny, J., & Meyer, G. (2012). Computer rendering and visual detection of orange peel. *Journal of Coatings Technology and Research, 9*(3), 297–307. https://doi.org/10.1007/s11998-011-9378-2
14. Peters, C. A., Nichols, M. E., & Ellwood, K. R. J. (2011). The evolution of surface texture in automotive coatings. *Journal of Coatings Technology and Research, 8*(4), 469–480. https://doi.org/10.1007/s11998-011-9333-2
15. Oba, Y., & Kakinuma, Y. (2017). Simultaneous tool posture and polishing force control of unknown curved surface using serial-parallel mechanism polishing machine. *Precision Engineering, 49*, 24–32. https://doi.org/10.1016/j.precisioneng.2017.01.006
16. Oba, Y., Yamada, Y., Igarashi, K., Katsura, S., & Kakinuma, Y. (2016). Replication of skilled polishing technique with serial-parallel mechanism polishing machine. *Precision Engineering, 45*, 292–300. https://doi.org/10.1016/j.precisioneng.2016.03.006
17. Brygo, F., Dutouquet, C., Le Guern, F., Oltra, R., Semerok, A., & Weulersse, J. M. (2006). Laser fluence, repetition rate and pulse duration effects on paint ablation. *Applied Surface Science, 252*(6), 2131–2138. https://doi.org/10.1016/j.apsusc.2005.02.143
18. Zhao, H. C., Qiao, Y. L., Zhang, Q., Du, X., Zang, Y., Liu, X. T., & Han, B. Y. (2020). Study on the characteristics and mechanism of pulsed laser cleaning of polyacrylate resin coating on aluminum alloy substrates. *Applied Optics, 59*(23), 7053–7065. https://doi.org/10.1364/AO.387532
19. Veltrup, M., Lukasczyk, T., Ihde, J., & Mayer, B. (2018). Distribution and avoidance of debris on epoxy resin during UV ns-laser scanning processes. *Applied Surface Science, 440*, 1107–1115. https://doi.org/10.1016/j.apsusc.2018.01.154
20. Lippert, T., Hauer, M., Phipps, C. R., & Wokaun, A. (2003). Fundamentals and applications of polymers designed for laser ablation. *Applied Physics A: Materials Science & Processing, 77*, 259–264. https://doi.org/10.1007/s00339-003-2111-y
21. Kumar, A., Prasad, M., Shail, S., Bhatt, R. B., Behere, P. G., Afzal, M., Kumar, A., Kar, R., Nilaya, J. P., & Biswas, D. J. (2015). Pulsed laser-assisted removal of powder coating from galvanised steel surface: A characterisation study. *Applied Physics*

A: Materials Science and Processing, 119(3), 853–858. https://doi.org/10.1007/s00339-015-9050-2
22. Li, X., Zhang, Q., Zhou, X., Zhu, D., & Liu, Q. (2018). The influence of nanosecond laser pulse energy density for paint removal. *Optik, 156*, 841–846. https://doi.org/10.1016/j.ijleo.2017.11.010
23. Shamsujjoha, M., Agnew, S. R., Melia, M. A., Brooks, J. R., Tyler, T. J., & Fitz-Gerald, J. M. (2015). Effects of laser ablation coating removal (LACR) on a steel substrate: Part 1: Surface profile, microstructure, hardness, and adhesion. *Surface & Coatings Technology, 281*, 193–205. https://doi.org/10.1016/j.surfcoat.2015.01.071
24. Shamsujjoha, M., Agnew, S. R., Brooks, J. R., Tyler, T. J., & Fitz-Gerald, J. M. (2015). Effects of laser ablation coating removal (LACR) on a steel substrate: Part 2: Residual stress and fatigue. *Surface and Coatings Technology, 281*, 206–214. https://doi.org/10.1016/j.surfcoat.2015.02.034
25. Kreutz, E. W., Frerichs, H., Stricker, J., & Wesner, D. A. (1995). Processing of polymer surfaces by laser radiation. *Nuclear Instruments and Methods in Physics Research Section B: Beam Interactions with Materials and Atoms, 105*, 245–249. https://doi.org/10.1016/0168-583X(95)00539-0
26. Jang, P. R., Kim, C. G., Han, G. P., Ko, M. C., Kim, U. C., & Kim, H. S. (2019). Influence of laser spot scanning speed on micropolishing of metallic surface using UV nanosecond pulse laser. *International Journal of Advanced Manufacturing Technology, 103*, 423–432. https://doi.org/10.1007/s00170-019-03559-8
27. Yan, J., & Kobayashi, F. (2013). Laser recovery of machining damage under curved silicon surface. *CIRP Annals—Manufacturing Technology, 62*, 199–202. https://doi.org/10.1016/j.cirp.2013.03.109
28. Kobayashi, T., Sera, H., Wakabayashi, T., Endo, H., Takushima, Y., & Yan, J. (2018). Surface flattening and nanostructuring of steel by picosecond pulsed laser irradiation. *Nanomanufacturing and Metrology, 1*(4), 217–224. https://doi.org/10.1007/s41871-018-0023-x
29. Hamad, A. H. (2016). Effects of different laser pulse regimes (nanosecond, picosecond and femtosecond) on the ablation of materials for production of nanoparticles in liquid solution. In R. Viskup (Ed.), *High energy and short pulse lasers* (pp. 305–325). IntechOpen. https://doi.org/10.5772/57353
30. Guo, B., Sun, J., Hua, Y., Zhan, N., Jia, J., & Chu, K. (2020). Femtosecond laser micro/nano-manufacturing: Theories, measurements, methods, and applications. *Nanomanufacturing and Metrology, 3*, 26–67. https://doi.org/10.1007/s41871-020-00056-5

Ayumi Nakajima received her bachelor's degree in Mechanical Engineering from Keio University, Japan in 2020. She is currently a master's degree student in Mechanical Engineering at Keio University under supervision of Prof. Jiwang Yan. Her research interests include laser processing and micro/nano manufacturing.

Jiwang Yan received his Ph.D. from Tohoku University, Japan in 2000 and is currently a professor of Mechanical Engineering at Keio University (2012-now), leading the Laboratory for Precision Machining and Nano Processing. His research areas include ultraprecision machining, micro/nano manufacturing, laser processing, nanomaterials and nanomechanics.